

Crystallization morphology and self-assembly of polyacrylamide solutions during evaporation

Jun Hu^{1,2}, Zhan-Long Wang^{1,*}

¹Shenzhen Institute of Advanced Technology, Chinese Academy of Sciences, Shenzhen, Guangdong 518000, China.

²China University of Political Science and Law, Beijing, 100091, China.

*Author to whom correspondence should be addressed: zl.wang1@siat.ac.cn

Abstract:

This study investigated crystallization and self-assembly phenomena in polyacrylamide (PAM) solutions during evaporation. As the solvent gradually evaporated, microscopic crystals began to form in the solution. The results show that concentration gradients form as the solution evaporates, leading to varied crystalline morphologies. From the edge to the center of the PAM solution, grass-like structures with intricate vein-like patterns and irregular morphologies were formed. The concentration gradient played a crucial role in this process. The relationship between the concentration gradient and crystalline structures was elucidated using absorbance spectroscopy. Schematics and absorbance spectra illustrate the evolution of the crystallization stages. Our findings not only contribute to a fundamental understanding of colloidal self-assembly but also hold significant implications for various applications, including thin-film fabrication, drug delivery, and nanotechnology.

1. Introduction

Polymer films have gained significant attention because of their wide range of applications in various industries such as electronics, membranes, coatings, and sensors^[1-5]. The crystallization, self-assembly, and resulting patterning of these films play crucial roles in determining their properties and performance^[6-11]. Evaporation of a polymer solution is an important method for fabricating polymer films^[12-15]. Generally, by controlling the concentration of polymer solutions, volatility of solvents, evaporation rate, and other parameters, the deposition of polymers and formation of thin films can be effectively achieved^[12,13,16-19]. Examples include the preparation of self-assembled and coated films. In the preparation of self-assembled thin films, polymers are mixed with solvents to form a solution, and the concentration of the polymers in the solution is controlled through solvent evaporation to allow self-assembly into thin films^[20,21]. Self-assembled films can be prepared using polymers such as polyacrylic acid or polystyrene in organic solvents. The solution evaporation method is commonly used to prepare coated films. In this method, a polymer solution is coated onto the substrate, and the polymer is then deposited and formed into a thin film through solvent evaporation^[22]. This method is also used to prepare transparent conductive films such as zinc oxide or polymer conductive films^[23,24]. Electrospinning is a method of spinning polymer solutions into fibers using electrostatic forces, and the evaporation of the solution is a key step in the spinning process. After the polymer solution passes through the spinning nozzle, the solvent evaporates, and the polymer is deposited to form a thin fiber film^[25]. Electrospinning can be used to prepare nanofiber films such as polyesters, polyamides, and polypropylene. Solution drop coating is a simple method of preparing polymer films in which an appropriate amount of polymer solution is dropped onto the substrate, and the polymer in the solution forms a thin film through solvent evaporation^[22]. Films prepared by solution drop coating are used to prepare organic optoelectronic devices, sensors, and thin-film substrates. Therefore, the evaporation of polymer solutions is important in many cutting-edge research fields.

Extensive research has been conducted globally in the field of thin film formation by polymer solution evaporation, leading to significant advancements. Researchers have explored various methods such as spin coating, drop casting, and immersion to achieve uniform evaporation and thin-film formation of polymer solutions^[22,26]. The influence of various solution parameters, including

the polymer concentration, evaporation rate, and characteristics of additives and solvents, on the morphology and properties of the films has been investigated [12,13,16-19]. Significant progress has been made in studying the structure, thickness, and surface morphology as well as mechanical, optical, and electrical properties of films and exploring ways to control the film structure and properties through polymer solution evaporation [27,28]. Polymer films formed by solution evaporation have been applied in diverse fields, including optoelectronic devices (such as solar cells), sensors, flexible electronics, and biomedicine [29,30]. Fundamental research on these mechanisms involves studying the behavior of liquid droplets, interfacial phenomena, and mass transfer during polymer solution evaporation, with the aim of gaining a deeper understanding of the underlying principles of thin film formation [18,31-36]. In terms of scaling up and process optimization, researchers are dedicated to achieving large-scale production of polymer solution-evaporated films while improving process reproducibility and efficiency and exploring optimized process conditions to enhance film quality and performance. These research areas focus on understanding the mechanisms that control the morphology, tune the properties, and expand the applications of polymer solution-evaporated films, thereby providing a foundation for the development of this technology. However, despite significant progress in understanding the mechanisms, applications, performance, and evaporation patterns of polymer solution-evaporated films, numerous phenomena and issues remain unresolved in this field.

Polyacrylamide (PAM) is an important synthetic polymer with a high molecular weight, high water absorption, excellent stability, ecological friendliness, and other characteristics. PAM is widely used in water treatment, thickeners, colloid stabilizers, oil mining, textile and paper industries, hydrogel materials and their applications, and many other fields [37,38]. PAM has a high molecular weight, which provides good solubility and viscosity. PAM also exhibits good water absorption and can rapidly form gels in water. In addition, PAM has excellent chemical and thermal stability and can maintain its performance and extend its service life under various environmental conditions. These characteristics have attracted considerable attention and applications. Key research topics regarding PAM include its formation of aqueous solutions, viscosity, and formation of thin films.

In this study, we focused on the different crystal morphologies and self-assembly phenomena formed by the evaporation of the PAM solution thin film formation. We conducted experiments using PAM solutions at concentrations of 1%, 2%, and 5% and examined their drying behavior in transparent plastic culture dishes. Through visual observation, we characterized the crystallization patterns that emerged after solvent evaporation. The crystallization of the PAM solution showed three stages: a chaotic particle pattern from the center to the edge, a mountain pattern, and a grass-like pattern. This phenomenon can be attributed to the induction of concentration changes generated by internal flow fields during evaporation. The absorption spectrum indicated that during the evaporation of the solution, the non-dried portion gradually increased with the evaporation concentration. This work reveals a new phenomenon of polymer solution crystallization and self-assembly, which may expand our understanding of polymer solution crystallization and provide guidance for thin film preparation.

2. Materials and methods

The solutions were prepared by mixing the PAM powder and DI water at mass ratios of 1:99, 1:49, and 1:19 (mass percentages of 1%, 2%, and 5%, respectively). The PAM powder was purchased from the Shanghai Aladdin Company and had a molecular weight range from 4000 to 40000. The steps for preparing the PAM solution are as follows. First, the corresponding volume of deionized water was added to a 100 ml beaker to ensure an adequate amount of solvent for dissolving the PAM powder. PAM powder was then slowly added during stirring to prevent powder agglomeration. The stirring speed was set to 800 rpm, and the mixture was stirred for 2 h to ensure the complete dissolution of PAM and obtain a homogeneous solution. Subsequently, the solution was inspected for clarity, and no suspended particles or lumps were observed. The prepared solutions are shown in Fig. 1b. The viscosity of the PAM solutions increased with increasing concentrations of the PAM powder. The PAM solution droplets were deposited on culture dishes. The volume of the PAM solution was reduced to 5 ml, and subsequently, the solution evaporated spontaneously and dried at room temperature to form a crystalline pattern. The room temperature was 25 °C, and the relative humidity was maintained at 60%.

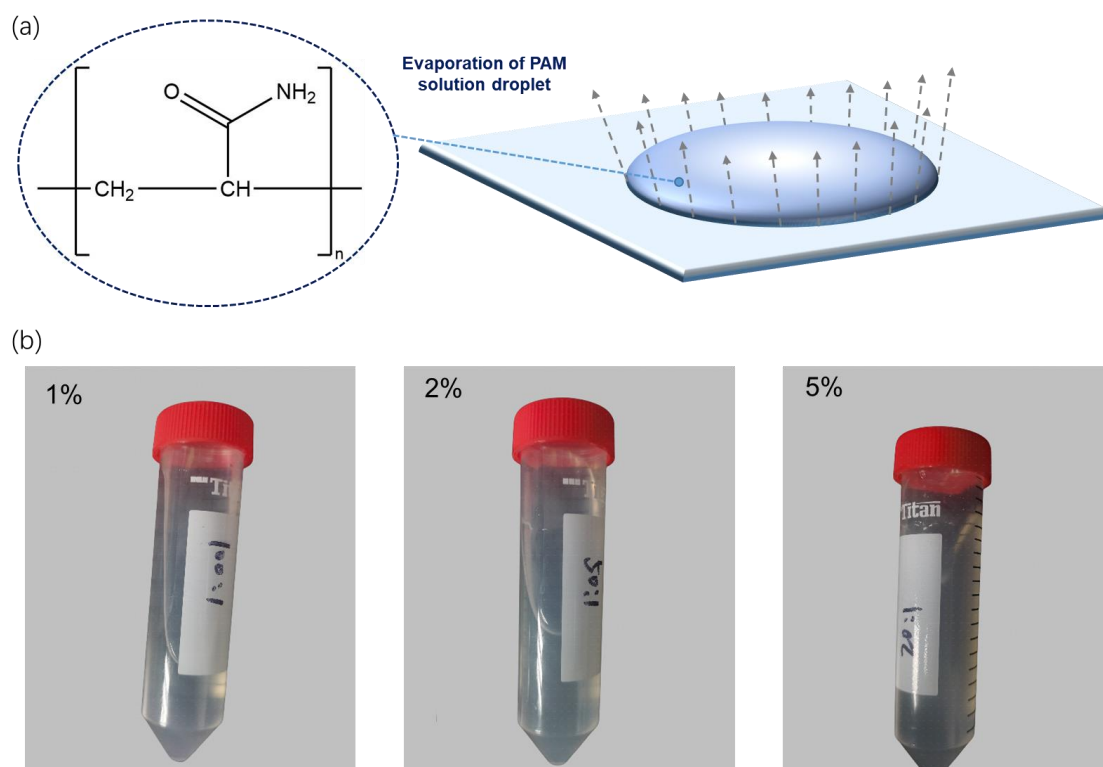


Figure 1. (a) The diagram of PAM solution droplet evaporation; (b) the prepared mixed PAM solutions.

3. Results and discussion

In Fig. 2, the drying behavior of PAM solutions at 1%, 2%, and 5% concentrations in transparent plastic Petri dishes with a diameter of 3.5 mm is presented. Figure 2a–c represent the 1%, 2%, and 5% concentrations, respectively. For the 1% solution in Fig. 2a, as the solvent evaporated, the PAM solution formed a nonuniform thin film. This crystalline morphology suggests that the polymer molecules in the 1% PAM solution arranged in an ordered manner during drying, resulting in a tightly packed structure. In the case of the 2% solution, as shown in Fig. 2b, distinct structural differences were observed among the three different regions of the dried crystalline morphology. This indicates that significant variations in the crystallization process occurred within different regions of the 2% solution. These local morphological differences may be attributed to concentration gradients and differences in the arrangement of the polymer molecules in different concentration regions. In contrast, the 5% solution exhibited two distinct crystalline morphologies upon drying, as shown in Fig. 2c. This could be due to the formation of local concentration gradients under high-concentration conditions, leading to variations in the crystallization behavior in different regions. Consequently, two different crystalline morphologies were formed. Among these observations, the 2% solution displayed the clearest crystalline pattern. This may be attributed to the fact that at

moderate concentrations, the arrangement of polymer molecules is better controlled, resulting in the formation of a more ordered structure during crystallization. In contrast, the 1% and 5% solutions did not exhibit evident crystalline patterns, possibly because of the difficulty in crystallizing at low or high concentrations, leading to challenges in forming a uniform structure.

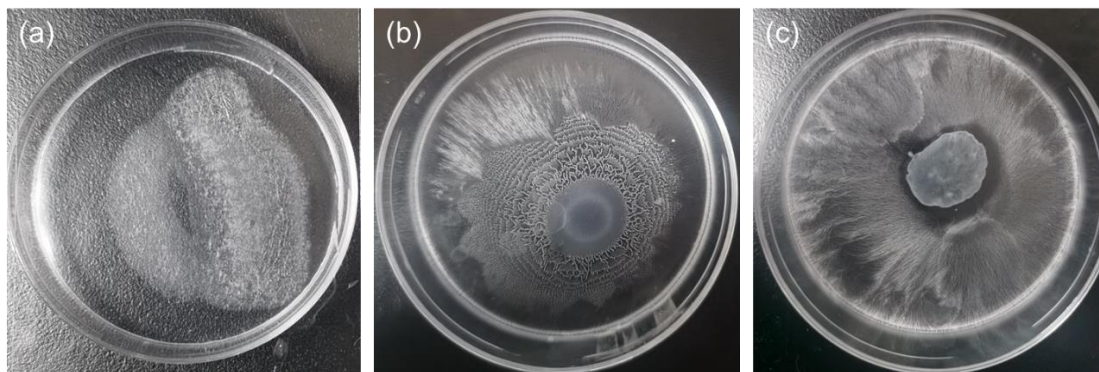


Figure 2. Images of the patterning during PAM solution evaporation in plastic culture dishes. (a)–(c) show the crystalline morphology formed by drying 1%, 2%, and 5% PAM solutions in culture dishes, respectively.

Evaporation-induced crystallization of the 2% PAM solution in plastic Petri dishes resulted in the formation of intricate crystal morphologies, as shown in Fig. 3. Figure 3a illustrates three distinct morphologies that expand outward from the center. At the center, disordered granular crystals were observed, representing the first level of crystallization. Surrounding the granular crystals, in the second level of crystallization, a network resembling mountain ridges emerged, with intercalated petal-like structures. Furthermore, in the third level of crystallization, independent grass-like crystal textures were formed, exhibiting branch-like or feather-like morphologies. Figure 3 illustrates this phenomenon, depicting the macroscopic and microscopic morphologies. Figure 3a shows macroscopic images of the three morphology levels. Figure 3b shows the microscopic view of the central first-level morphology, while Fig. 3c shows the microscopic morphology of the transition region from the first to the second level. Figure 3d shows the microscopic morphology of the second-level ridge-like textures, and Fig. 3e shows the microscopic morphology at the junction of the second and third levels. Finally, Fig. 3f shows the microscopic morphology of the third-level grass- or branch-like structures.

Figure 3 shows the change in the crystal morphology during the evaporation of the PAM solution. This complex crystallization behavior can be attributed to several factors. The concentration of the PAM solution plays a critical role in determining the resulting morphology. The 2% concentration

used in this study favored the formation of hierarchical structures owing to the interplay of polymer-solvent interactions and solvent evaporation kinetics. As the solvent evaporated, the polymer molecules underwent self-assembly, leading to the observed hierarchical organization. In addition, the kinetics of solvent evaporation contributed significantly to the formation of diverse morphologies. The spatial variation in evaporation rates across the Petri dish surface led to differential concentration gradients, influencing the nucleation and growth of crystals. This results in the formation of distinct morphological features such as granular clusters, ridge-like networks, and grass structures. Furthermore, the interplay between the polymer chain mobility and solvent diffusion during evaporation governs the hierarchical assembly process. As solvent molecules escape, the polymer chains undergo conformational changes and aggregate to minimize free energy, giving rise to the observed multilevel morphologies. Among the numerous factors involved, solvent evaporation dynamics have emerged as a pivotal aspect shaping the complex crystallization behavior. Solvent evaporation dynamics encompass the interplay between the various processes that occur during solvent removal, such as diffusion, concentration gradients, and surface effects.

At the heart of solvent evaporation dynamics is the concentration gradient established as solvent molecules escape from the solution into the surrounding environment. This concentration gradient induces differential rates of solvent removal across the solution, leading to localized variations in the polymer concentration. These concentration variations influence the nucleation and growth processes, ultimately shaping the morphology of the formed crystalline structures. **Moreover**, the spatial and temporal variations in the solvent evaporation rates contribute to the formation of distinct regions within the crystallizing solution, each characterized by unique concentration profiles. These concentration gradients act as driving forces for the migration of the polymer chains, leading to the assembly of ordered structures at multiple length scales. The observed hierarchical organization, such as the formation of particle clusters, mountain-like networks, and branching structures, can be attributed to spatially heterogeneous solvent evaporation dynamics. **Furthermore**, the dynamics of the polymer chain motion are intricately linked to solvent evaporation. As solvent molecules escape, the polymer chains undergo conformational changes and self-assembly to minimize free energy. Competition between chain mobility and polymer-polymer interactions underlies the emergence of hierarchical structures during crystallization. Surface effects also occur as solvent molecules

evaporate more rapidly from the exposed surfaces of the solution, leading to enhanced polymer concentration gradients and localized crystallization. The confinement imposed by the container surface further influences the spatial distribution of the polymer chains, contributing to the formation of structured morphologies. **Solvent evaporation** dynamics have emerged as critical factors governing the complex crystallization behavior observed in PAM solutions. The establishment of concentration gradients, differential rates of solvent removal, polymer chain dynamics, and surface effects collectively drive the hierarchical assembly of the crystalline structures. Understanding and manipulating these dynamics offers avenues for tailoring the properties of crystalline materials across various length scales, with implications for applications in materials science, biotechnology, and beyond.

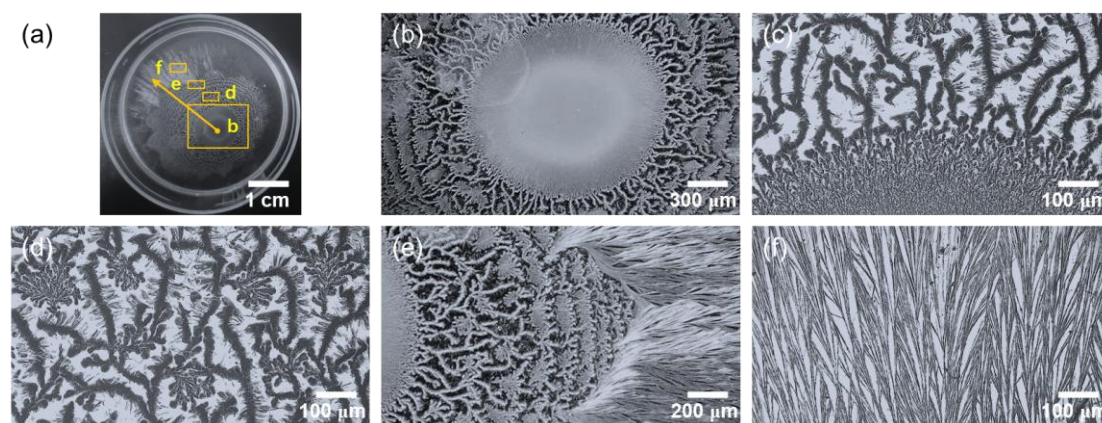


Figure 3. The microscopic images of the crystal morphology of PAM solutions in a culture dish. (a) The whole and macroscopic view of the solution crystal morphology. The crystal presents a three-stage gradient change. (b) The microscopic crystal morphology in the first stage in the center of culture dish. (c) The microscopic view of the crystal at the junction of the first and second stages. (d) The microscopic crystal morphology in the second stage. (e) The microscopic view of the crystal at the junction of the second and third stages. (f) The microscopic crystal morphology in the third stage.

In Fig. 4, we present the results of crystallization observed in the third stage, which is characterized by the formation of dendritic or grass-like structures within the PAM solution. These dendritic or grass-like crystals exhibit a characteristic morphology, with individual branches possessing widths of approximately $10\ \mu\text{m}$ and lengths ranging from $500\ \mu\text{m}$ to $1\ \text{mm}$. The overall appearance is a grass-like crystalline structure. Figure 4 shows micrographs of different regions of these crystals, highlighting their observed characteristics. Figure 4a shows an overview of the

overall morphology of the grass-like crystals formed by the crystallization of the PAM solutions. Figure 4b-d show details of the crystal morphology at different locations in the complete grass-like crystal. The formation of the dendritic and grass-like structures can be attributed to several factors. One of the contributing factors is the nucleation and growth kinetics of the solution. As the polymer solution cools or evaporates, localized regions with higher polymer concentrations can initiate the formation of nucleation sites. These sites serve as points for crystal growth, with polymer molecules aggregating and aligning along specific directions dictated by the intermolecular forces and chain conformations. The dendritic morphology arises from the preferential growth along certain crystallographic axes, resulting in branching structures. Furthermore, the presence of impurities or additives in the solution can influence the crystallization process. Impurities may act as heterogeneous nucleation sites, promoting the formation of crystals with nonuniform shapes and branching patterns. In addition, the interactions between the polymer and solvent molecules play a crucial role in determining the final morphology of the crystals. Variations in the solvent composition, temperature, and concentration gradients can affect the crystallization process, leading to the observed diversity in crystal morphology.

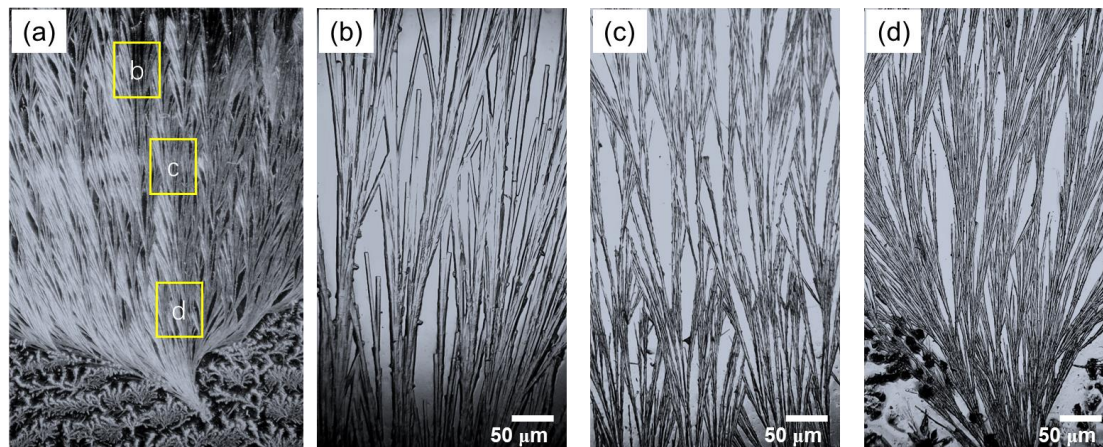


Figure 4. The tussock-like crystals formed in the third-level crystallization area. (a) The enlarged image of the grass-like crystal structures in the third level. (b) The microscopic view of the dendritic or grass-like structures in the tail section of the crystal. (c) The microscopic images in the middle section of the grass-like crystal structures. (d) The microscopic view of the grass-like crystal in the section near the crystal root.

In Fig. 5, we observe the crystallization patterns in the second stage, which are characterized by the formation of mountainous vein-like structures. These crystals exhibit irregular vein textures with widths of approximately 10 μm , and gaps exist between the veins where petal-shaped crystals are

generated. Micrographs of different regions of these crystals clearly show these observed characteristics (Fig. 5a–f). The formation of these mountainous vein-like structures in the PAM solution can be attributed to multiple factors. The interplay among the polymer concentration, solvent evaporation rate, and temperature gradient within the solution is a key factor. As the solvent evaporates or the solution cools, the polymer molecules tend to aggregate and align along specific directions, leading to the formation of vein-like structures. Irregularities in the vein texture and the generation of petal-shaped crystals in the gaps between veins may be influenced by variations in the local polymer concentration, solvent composition, and presence of impurities. In addition, crystal growth dynamics play a crucial role in shaping the observed morphology. The growth of petal-shaped crystals in the gaps between the veins may have resulted from the preferential attachment of polymer molecules to these sites, leading to the formation of distinctive features. Furthermore, irregular vein textures could arise from variations in the growth rates along different directions, indicating a complex interplay of kinetic and thermodynamic factors during crystallization.

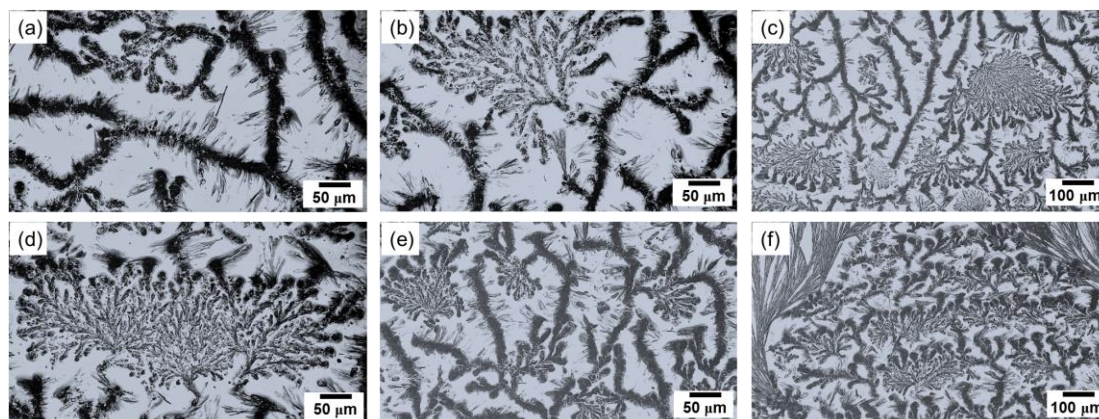


Figure 5. The veined crystals forming in the second-level crystallization area. (a)–(f) Different views of the veined crystals.

Figure 6 sheds light on the crystallization phenomena observed in Figs. 3 to 5 and delves into their underlying mechanisms. Absorbance spectroscopy analysis reveals a gradual increase in solution concentration during the PAM solution evaporation process. This concentration gradient, with lower concentrations at the periphery and higher concentrations towards the center, contributes to the formation of the tri-level structure depicted in Fig. 3. Panels a to f of Fig. 6 depict schematic diagrams of evaporation stages and absorbance spectra. Panel a corresponds to the initial evaporation stage, showcasing the formation of the third-level grass-like crystalline structure

observed in Fig. 3. Panel b illustrates an intermediate stage of evaporative crystallization, where increasing solution concentration leads to the formation of the second-level mountainous vein-like crystalline structure. Ultimately, a further increase in solution concentration results in the formation of the first-level irregular evaporative crystal morphology. The absorbance spectra depicted in panels d, e, and f exhibit a consistent trend of increasing absorbance intensity, indicating a gradual rise in solution concentration. This observation aligns with the presence of concentration gradients observed during the evaporation process, which play a pivotal role in shaping the intricate crystalline structures depicted in Figs. 3 to 5. Through this systematic examination of the evaporation process and its correlation with solution concentration, valuable insights are gained into the mechanisms dictating the formation of complex crystalline morphologies within the PAM solution. By elucidating the relationship between concentration gradients and crystallization behavior, this analysis deepens our understanding of the intricate interplay between thermodynamic and kinetic factors governing polymer crystallization processes.

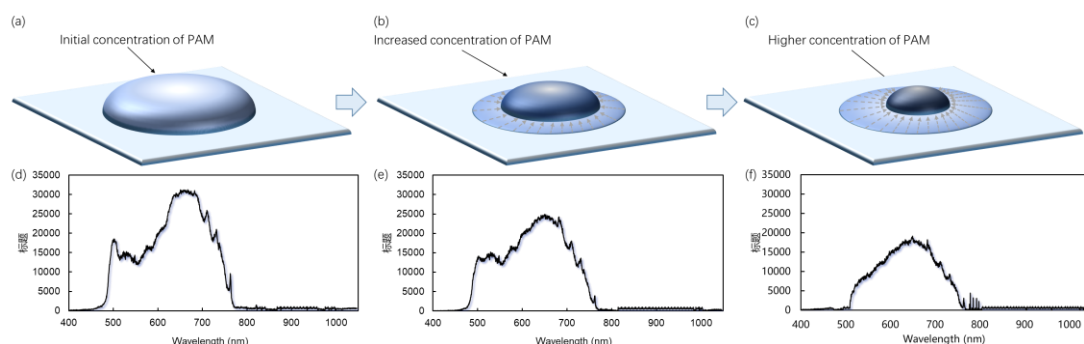


Figure 6. Diagram of the mechanism of PAM solution evaporation on a solid surface. (a)–(c) Diagram of the progress of PAM solution evaporation. As the PAM solution evaporates, the concentration of the residual solution increases under the internal flow fields. (d)–(f) The absorption spectrograms of the solutions in different stages. The spectrograms show that the absorption intensity gradually increases as the PAM solution evaporates.

4. Conclusions

This study explored the crystallization phenomena of PAM solutions during solution evaporation and thin-film formation. As the solution evaporates, the concentration gradually increases, leading to a concentration gradient across the solution. At the periphery, where evaporation initiates, the concentration remains relatively low, whereas towards the center, where evaporation persists, the concentration increases progressively. This concentration disparity contributes to the formation of

intricate crystalline structures. In addition, a comprehensive illustration of the evaporation process and its correlation with the solution concentration is provided through schematic diagrams and absorbance spectra. The results illustrate the initial stage of evaporation, which corresponds to the formation of a third-level grass-like crystalline structure. In the intermediate stage, the increasing solution concentration results in the formation of second-level mountainous vein-like crystalline structures. In the central section, the highest concentration leads to the formation of an irregular evaporative crystalline morphology. The absorbance spectra consistently show increasing absorbance intensity from the initial to final stages, indicating a progressive increase in the solution concentration. This supports the concentration gradients observed during evaporation, which influenced the formation of complex crystalline morphologies. Overall, this study provides valuable insights into the interplay between concentration gradients and crystallization behavior in PAM solutions during evaporation, enhances our understanding of the underlying mechanisms governing polymer crystallization processes, and contributes to advancements in various fields, including materials science, pharmaceuticals, and nanotechnology.

Acknowledgment:

This work was supported by the National Natural Science Foundation of China (No. 12202461), Shenzhen Science and Technology Research Program (Grant JCYJ20210324101610028)

Conflict of Interest

The authors have no conflicts to disclose

References:

- [1] A. H. Gelebart, D. Jan Mulder, M. Varga, et al. Making waves in a photoactive polymer film. *Nature* **546** (2017) 632-636.
- [2] Y. Xu, D. Kraemer, B. Song, et al. Nanostructured polymer films with metal-like thermal conductivity. *Nat. Commun.* **10** (2019) 1771.
- [3] D. Li, X. Liu, W. Li, et al. Scalable and hierarchically designed polymer film as a selective thermal emitter for high-performance all-day radiative cooling. *Nat. Nanotechnol.* **16** (2021) 153-158.
- [4] D. Q. Tan. Review of polymer-based nanodielectric exploration and film scale-up for advanced capacitors. *Adv. Funct. Mater.* **30** (2019).
- [5] J. Xu, H. C. Wu, C. Zhu, et al. Multi-scale ordering in highly stretchable polymer semiconducting films. *Nat. Mater.* **18** (2019) 594-601.
- [6] R. M. Michell and A. J. Müller. Confined crystallization of polymeric materials. *Prog. Polym. Sci.* **54-55**

- (2016) 183-213.
- [7] M. Zhang, B.-H. Guo and J. Xu. A review on polymer crystallization theories. *Crystals* **7** (2016) 4.
- [8] K. Dey, M. Pal, K. C. Rout, et al. Selective molecular separation by interfacially crystallized covalent organic framework thin films. *J. Am. Chem. Soc.* **139** (2017) 13083-13091.
- [9] K. Thorkelsson, P. Bai and T. Xu. Self-assembly and applications of anisotropic nanomaterials: A review. *Nano Today* **10** (2015) 48-66.
- [10] M. Stefik, S. Guldin, S. Vignolini, et al. Block copolymer self-assembly for nanophotonics. *Chem. Soc. Rev.* **44** (2015) 5076-5091.
- [11] D. Di Nuzzo, C. Kulkarni, B. Zhao, et al. High circular polarization of electroluminescence achieved via self-assembly of a light-emitting chiral conjugated polymer into multidomain cholesteric films. *ACS Nano* **11** (2017) 12713-12722.
- [12] G. A. Zoumpouli and S. G. Yiantsios. Hydrodynamic effects on phase separation morphologies in evaporating thin films of polymer solutions. *Phys. Fluids* **28** (2016).
- [13] C. Schaefer, P. van der Schoot and J. J. Michels. Structuring of polymer solutions upon solvent evaporation. *Phys Rev E Stat Nonlin Soft Matter Phys* **91** (2015) 022602.
- [14] D. Khim, G. S. Ryu, W. T. Park, et al. Precisely controlled ultrathin conjugated polymer films for large area transparent transistors and highly sensitive chemical sensors. *Adv. Mater.* **28** (2016) 2752-2759.
- [15] K. H. Ku, J. M. Shin, H. Yun, et al. Multidimensional design of anisotropic polymer particles from solvent-evaporative emulsion. *Adv. Funct. Mater.* **28** (2018).
- [16] T. Okuzono, K. Ozawa and M. Doi. Simple model of skin formation caused by solvent evaporation in polymer solutions. *Phys. Rev. Lett.* **97** (2006) 136103.
- [17] E. Bormashenko, R. Pogreb, A. Musin, et al. Self-assembly in evaporated polymer solutions: Influence of the solution concentration. *J. Colloid Interface Sci.* **297** (2006) 534-540.
- [18] C. Schaefer, J. J. Michels and P. van der Schoot. Structuring of thin-film polymer mixtures upon solvent evaporation. *Macromolecules* **49** (2016) 6858-6870.
- [19] E. Bormashenko, R. Pogreb, O. Stanevsky, et al. Mesoscopic patterning in evaporated polymer solutions: New experimental data and physical mechanisms. *Langmuir* **21** (2005) 9604-9609.
- [20] S. A. DiBenedetto, A. Facchetti, M. A. Ratner, et al. Molecular self-assembled monolayers and multilayers for organic and unconventional inorganic thin-film transistor applications. *Adv. Mater.* **21** (2009) 1407-1433.
- [21] H. S. Lee, D. H. Kim, J. H. Cho, et al. Effect of the phase states of self-assembled monolayers on pentacene growth and thin-film transistor characteristics. *J. Am. Chem. Soc.* **130** (2008) 10556-10564.
- [22] A. Münch, C. P. Please and B. Wagner. Spin coating of an evaporating polymer solution. *Phys. Fluids* **23** (2011).
- [23] H. C. Chen, S. W. Lin, J. M. Jiang, et al. Solution-processed zinc oxide/polyethylenimine nanocomposites as tunable electron transport layers for highly efficient bulk heterojunction polymer solar cells. *ACS Appl. Mater. Interfaces* **7** (2015) 6273-6281.
- [24] K. J. Loh and D. Chang. Zinc oxide nanoparticle-polymeric thin films for dynamic strain sensing. *J. Mater. Sci.* **46** (2010) 228-237.
- [25] X. H. Li, C. L. Shao and Y. C. Liu. A simple method for controllable preparation of polymer nanotubes via a single capillary electrospinning. *Langmuir* **23** (2007) 10920-10923.
- [26] M. Eslamian and F. Soltani-Kordshuli. Development of multiple-droplet drop-casting method for the fabrication of coatings and thin solid films. *J. Coat. Technol. Res.* **15** (2017) 271-280.
- [27] J. M. Torres, C. Wang, E. B. Coughlin, et al. Influence of chain stiffness on thermal and mechanical

- properties of polymer thin films. *Macromolecules* **44** (2011) 9040-9045.
- [28] H. S. Abdulla and A. I. Abbo. Optical and electrical properties of thin films of polyaniline and polypyrrole. *Int. J. Electrochem. Sci.* **7** (2012) 10666-10678.
- [29] J. Zhao, Z. Chi, Z. Yang, et al. Recent developments of truly stretchable thin film electronic and optoelectronic devices. *Nanoscale* **10** (2018) 5764-5792.
- [30] X. Wu and H. Peng. Polymer-based flexible bioelectronics. *Sci Bull (Beijing)* **64** (2019) 634-640.
- [31] Z. Wang, X. Wang, Q. Miao, et al. Realization of self-rotating droplets based on liquid metal. *Adv. Mater. Interfaces* **8** (2020) 2001756.
- [32] Z. Wang, X. Wang, Q. Miao, et al. Spontaneous motion and rotation of acid droplets on the surface of a liquid metal. *Langmuir* **37** (2021) 4370-4379.
- [33] Z.-L. Wang and K. Lin. The multi-lobed rotation of droplets induced by interfacial reactions. *Phys. Fluids* **35** (2023) 021705.
- [34] Z. Wang, E. Chen and Y. Zhao. The effect of surface anisotropy on contact angles and the characterization of elliptical cap droplets. *Sci. China Technol. Sc.* **61** (2017) 309-316.
- [35] Z. Wang and Y. P. Zhao. Wetting and electrowetting on corrugated substrates. *Phys. Fluids* (2017).
- [36] J. Cummings, J. S. Lowengrub, B. G. Sumpter, et al. Modeling solvent evaporation during thin film formation in phase separating polymer mixtures. *Soft Matter* **14** (2018) 1833-1846.
- [37] K. Godwin Uranta, S. Rezaei-Gomari, P. Russell, et al. Studying the effectiveness of polyacrylamide (pam) application in hydrocarbon reservoirs at different operational conditions. *Energies* **11** (2018) 2201.
- [38] A. K. Dunker and R. R. Rueckert. Observations on molecular weight determinations on polyacrylamide gel. *J. Biol. Chem.* **244** (1969) 5074-5080.